

Electromagnetic Interference (EMI) Shielding Performance of the Ternary Composite Based on BaFe₁₂O₁₉, MWCNT and PANI at the Ku-Band

Muhammad H. Zahari¹, Beh H. Guan^{1, *}, Ee M. Cheng²,
Muhammad F. Che Mansor³, and Hazliza A. Rahim⁴

Abstract—A ternary composite, based on the M-type hexagonal barium ferrite, BaFe₁₂O₁₉, conducting polymer, polyaniline (PANI), carbon allotrope, and multi-walled carbon nanotube (MWCNT), was prepared through a facile *in-situ* polymerization process. The structural properties of the synthesized composites were characterized through XRD and FESEM analysis. PANI particles were found to be able to coat on BaFe₁₂O₁₉ and MWCNT surfaces. The increased MWCNT wt% loading within the composite resulted in the increase of the electrical conductivity with values as high as 2.0320 S/m for sample PBM5 (25wt% MWCNT). The composite inherited the salient properties of its respective components to achieve optimum values of shielding effectiveness. The highest value of SE_A recorded was 42.37 dB at 17.60 GHz. The significantly larger magnitudes of SE_A than SE_R suggest that the mechanism of shielding for all synthesized composites are through absorption.

1. INTRODUCTION

Electromagnetic interference (EMI) is a form of pollution that exists as a side-effect of the rapid development of digital devices and communication technology. Modern day devices, especially those involving signal transmission and reception, are potential victims of the pollution which can cause problems, from as minor as static noises and signal degradations to much severe cases such as data loss, signal interception and device failure if left unattended. The methods of protection against unwanted EMI emission mainly falls under two categories; intelligent circuit design and shielding. Ideally, an intelligent circuit design is much preferred as the problem can be addressed at a much earlier stage which enables electronic devices to possess better electromagnetic compatibility (EMC). However, there are numerous cases in which it is impossible to implement the intelligent circuit design due to hardware and economical limitations. For these cases, the utilization of shielding materials to block unwanted EMI transmission is a much practical practice [1].

A radiated electromagnetic wave incident upon the surface of a material with a different impedance would result in three main outcomes; reflection, absorption and transmission of the propagated wave. As the primary goal of a shielding material is to block the EMI, it is thus important to fine-tune the intrinsic properties such as the complex permittivity, ϵ_r , and complex permeability, μ_r , of the shielding materials, so as to enable optimum reflection and/or absorption. While there is no single material capable of fulfilling all of the criteria for optimum shielding at the same time, it is possible to combine

Received 4 October 2016, Accepted 8 November 2016, Scheduled 29 November 2016

* Corresponding author: Beh Hoe Guan (beh.hoeguan@utp.edu.my).

¹ Fundamental and Applied Sciences Department, Universiti Teknologi Petronas, 32610, Seri Iskandar, Perak Darul Ridzuan, Malaysia. ² School of Mechatronic Engineering, Universiti Malaysia Perlis (UniMAP), 02600 Arau, Perlis, Malaysia. ³ School of Material Engineering, Universiti Malaysia Perlis (UniMAP), 02600 Arau, Perlis, Malaysia. ⁴ Bioelectromagnetics Research Group (BioEM), School of Computer and Communication Engineering, Universiti Malaysia Perlis (UniMAP), 02600 Arau, Perlis, Malaysia.

various salient properties of different materials to form a competent hybrid shielding material. Hexagonal ferrites are an important class of ferrites known to be able to exhibit large values of permeability at GHz frequencies [2, 3]. Combined with its chemical stability [4] and good magnetic properties [5, 6], hexagonal ferrite is a promising candidate to be used as a shielding material. However, as it is a magnetic material, the main mechanism of loss would be magnetic (eddy current loss, hysteresis loss, etc.) As electromagnetic waves consist of both magnetic and electrical components travelling perpendicular to each other, another component needs to be introduced in order to produce dielectric losses. This can easily be done by using intrinsically conducting polymers such as polyaniline. Polyaniline is a polymer belonging to the unique class of conjugated polymer where its electrical conductivity is a product of acidic doping [7]. Properties such as light weight, resistance to corrosion and ease of processibility make it very appealing for its utilization as shielding materials [8, 9]. Another type of material known to exhibit good electrical properties is multi-walled carbon nanotubes (MWCNT) [10]. With adequate dispersion and amounts in composites, MWCNTs are known to show promising shielding capabilities when being paired with other shielding materials [11]. Its light weight would also help in offsetting the high density ferrite while still contributing towards the overall shielding performance.

In this research work, a hybrid composite material for EMI shielding applications is proposed. BaFe₁₂O₁₉ from the family of M-type hexagonal ferrite, carbon allotrope, MWCNT, conducting polymer, PANI, were brought together by a simple *in-situ* polymerization process, and the composite product was evaluated in terms of its structural, electrical and electromagnetic properties through x-ray diffraction (XRD) analysis, field-emission scanning electron microscope (FESEM) and *S*-parameter measurements. The effect of different MWCNT loadings, especially towards the shielding effectiveness, SE, was reported.

2. METHODS

The composite was synthesized through a facile *in-situ* polymerization of aniline alongside BaFe₁₂O₁₉ and multi-walled carbon nanotubes (MWCNT). The MWCNT (70–80% assay, *Sigma-Aldrich*) was procured readily while the ferrite was synthesized through a sol-gel combustion method as discussed in the next subsection.

2.1. Ferrite Synthesis

The nitrate precursors (99% purity, *R&M Chemicals*) of the ferrite were weighed according to the respective stoichiometric ratios to form the desired barium ferrite with the chemical formula of BaFe₁₂O₁₉ before being dissolved together in distilled water. Suitable amount of citric acid (99% purity, *R&M Chemicals*), with metal ion to citric acid ratio, 1 : 2, was added to chelate precursor materials followed by the addition of ammonia solution (~ 25%, *R&M Chemicals*) to bring the pH of the mixture to 7. The mixture was heated at 80°C and left to stir for 24 hours to obtain a concentrated, dark green gel. The obtained gel was directly combusted in a box furnace at 200°C for 30 minutes before being further calcined at 950°C for 3 hours. The ferrite synthesis process was then completed, and the ferrite was readily used in the composite synthesis process.

Table 1. Synthesized composites.

| Sample name | $x = (\text{wt}\%)$ |
|-------------|---------------------|
| PBM1 | 1 |
| PBM2 | 2 |
| PBM3 | 3 |
| PBM4 | 4 |
| PBM5 | 5 |

2.2. Composite Synthesis

The composite was synthesized based on the ratio formula, $(50-x/2)\text{BaFe}_{12}\text{O}_{19}:(50x/2)\text{Aniline}:(x)\text{MW-CNT}$, where x represents the amount of MWCNT within the composite. The different composites synthesized in this work are as listed in Table 1.

Required amounts of $\text{BaFe}_{12}\text{O}_{19}$ and MWCNT were mechanically stirred in distilled water for about 30 minutes before aniline (99% purity, *R&M Chemicals*), in 0.1M HCl, was added to the mixture. The stirring process was then done in an ice bath to bring the temperature of the mixture down to $\pm 3^\circ\text{C}$. Simultaneously, ammonium persulfate (APS) (99% purity, *R&M Chemicals*) solution, with aniline to APS ratio of 1 : 1.05, was cooled down to 0°C . The polymerization process starts as soon as the APS solution was added in drop-wise amounts to the $\text{BaFe}_{12}\text{O}_{19}$ -MWCNT-aniline mixture. The mixture was allowed to react for 6 hours, with continuous stirring and by maintaining the temperature at $\pm 3^\circ\text{C}$ throughout the whole reaction duration. The dark green mixture obtained at the end of the reaction was filtered and repeatedly washed with distilled water, followed by ethanol, until the filtrate becomes colourless. The wet substrate was finally dried in a drying oven at 80°C overnight, completing the composite synthesis.

2.3. Composite Characterization

X-ray diffraction (XRD) analysis was done on all synthesized composites by using a diffractometer (Bruker: D8 Advance RD) between the scanning angles of 20° and 90° . Surface micrographs of the samples were taken by using a FESEM LEO 1525, field-emission scanning electron microscope (FESEM) in order to investigate their morphological properties. Conductivity measurements were performed by using a 4-point resistivity measurement system (Keithley 2400). Electromagnetic measurements were conducted by utilizing a waveguide setup connected to a network analyser (Agilent Technologies E8362B) at the frequency range of 12–18 GHz, otherwise known as the Ku-band. To facilitate the measurement, the composites were mixed with paraffin wax in the ratio of 70 : 30 and then pressed into rectangular slabs with dimensions $22.86\text{ mm} \times 10.16\text{ mm} \times 4.5\text{ mm}$.

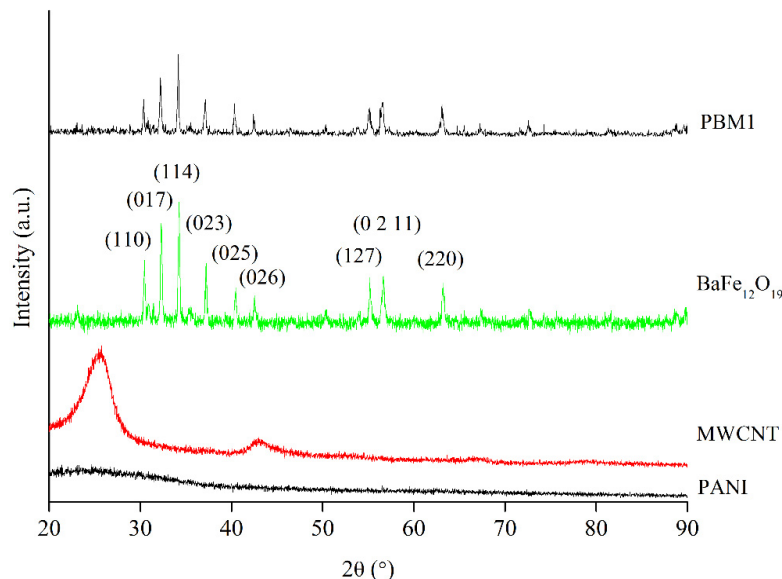


Figure 1. Comparison between the diffraction patterns of pure $\text{BaFe}_{12}\text{O}_{19}$, MWCNT and PANI with sample PBM1.

3. RESULTS AND DISCUSSIONS

The non-destructive nature of the polymer polymerization process suggests that there is no structural modification experienced by the other two constituents of the composite, $\text{BaFe}_{12}\text{O}_{19}$ and MWCNT. This was evidenced in Figure 1 which compares the diffraction patterns of one of the synthesized composites, PBM1, with the singular patterns of $\text{BaFe}_{12}\text{O}_{19}$, PANI and MWCNT.

As can be seen in Figure 1, prominent peaks of the crystallite material, $\text{BaFe}_{12}\text{O}_{19}$, are observed in sample PBM1 despite the mixing with the non-crystalline PANI and MWCNT. The characteristic peaks of PBM1 and $\text{BaFe}_{12}\text{O}_{19}$ match well to that obtained from a reference standard (ICSD98-010-6617). Peaks corresponding to the hkl indexes, (110), (017), (114), (023), (025), (026), (0211) and (220), were observed at scanning angles 30.35° , 32.17° , 34.14° , 37.11° , 40.31° , 42.45° , 56.50° and 63.11° , respectively. Despite the broad peak shown by the diffraction pattern of pure MWCNT, the peak was not observed in the composite sample. A possible reason for the observation is that the introduction of MWCNT leads

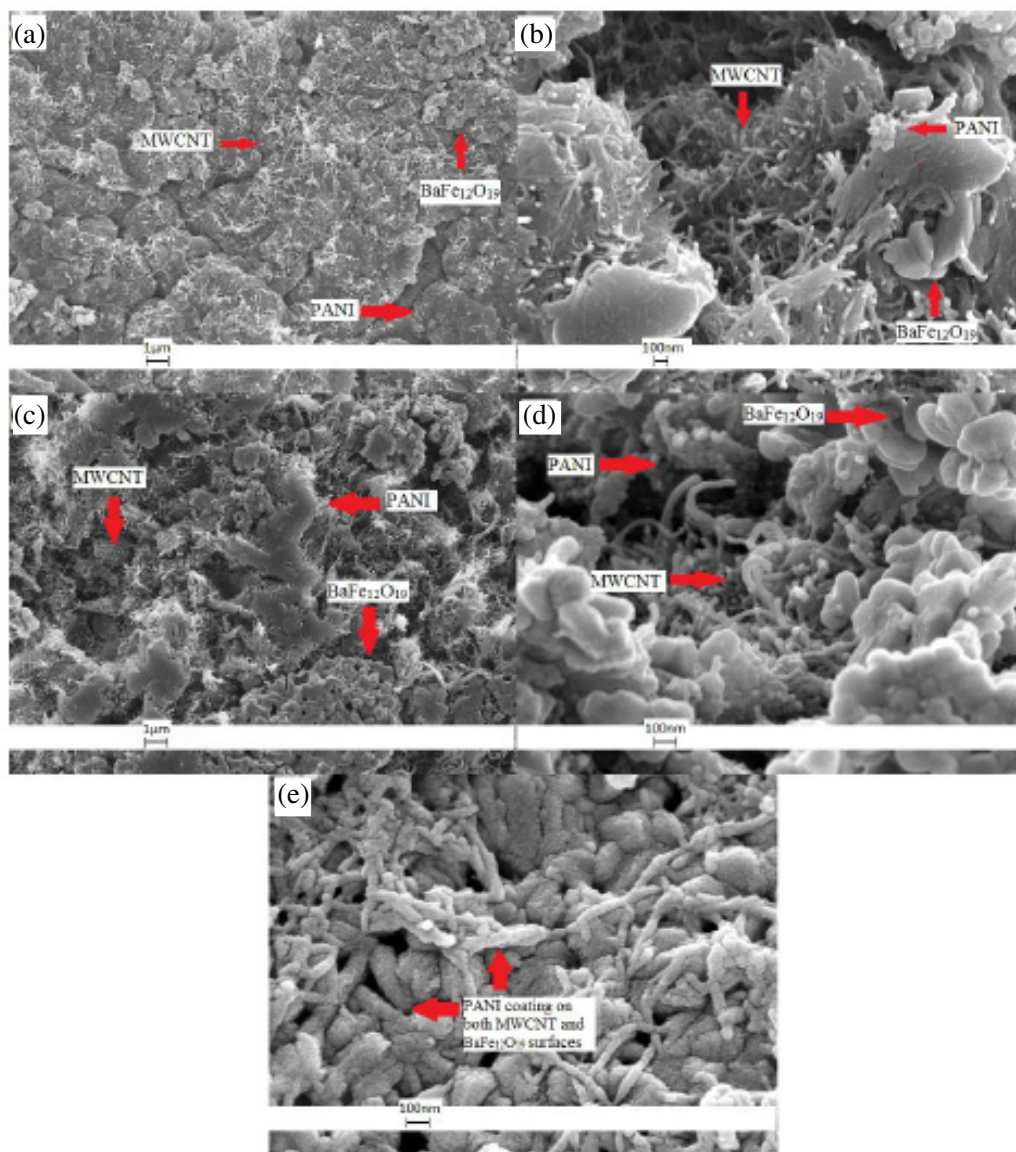


Figure 2. FESEM images of synthesized composites: (a) PBM1, (b) PBM2, (c) PBM3, (d) PBM4 and (e) PBM5.

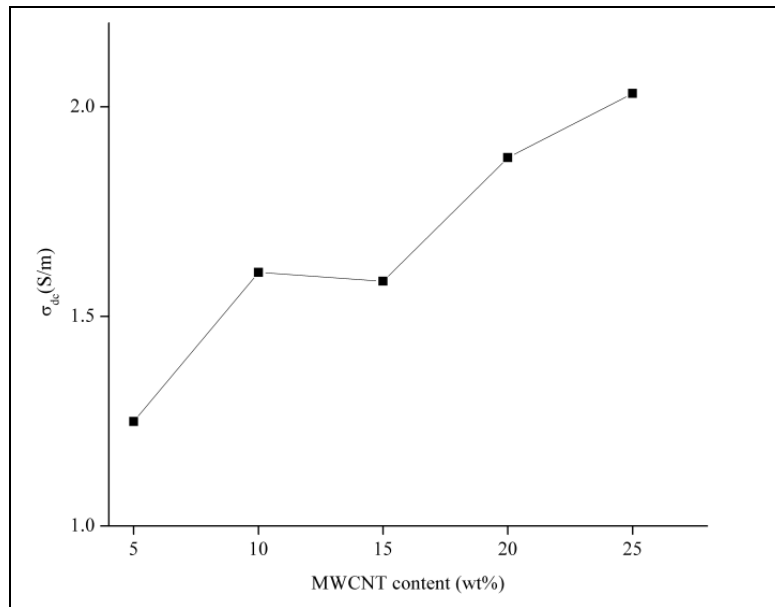


Figure 3. Effect of MWCNT content variation on the electrical conductivity of the synthesized composite.

to the increase in output of the polymer due to the higher surface area for the reaction [12]. This would also lead to a relative decrease in the $\text{BaFe}_{12}\text{O}_{19}$ content within the composite, causing the reduction in the peak intensity of the characteristic peaks attributed to the ferrite.

FESEM micrographs of the sample were taken at different focus sites in order to investigate the morphology and composite constituent distribution of the synthesized composite as shown in Figure 2. As can be seen in Figures 2(a)–(e), the particles of $\text{BaFe}_{12}\text{O}_{19}$ and MWCNT are seen randomly distributed throughout the composite powder with particles of PANI polymerizing on both surfaces. The ferrite grains consisting of large grain agglomerates are seen to possess a wide range of particle size distribution, between 60.52 nm and 457.60 nm, due to the nature of the chosen synthesis method [13]. This, combined with the high surface area of MWCNT, allows the possibility of PANI to form on both material surfaces, giving it a ‘coating’ form as seen in PBM5, in contrast with the tubular form normally attributed to PANI when the polymerization process takes place without the presence or contact with any foreign particles [14].

The effect of the different MWCNT loadings on the room temperature conductivity was investigated by using a 4-point probe resistivity measurement system, and the results are as illustrated in Figure 3. The increased MWCNT content results in the increase of the overall conductivity of the synthesized composites. A 5wt% MWCNT loading results in the measured conductivity of 1.2492 S/m. This further increased to 1.6049 S/m as the MWCNT content was further increased to 10wt% in sample PBM2. A slight drop (~ 0.02 S/m) in the electrical conductivity was observed for sample PBM3 which can be attributed to the sample inhomogeneity due to the nature of the synthesis process. However, further increase in the MWCNT continues to increase the electrical conductivity as the measured electrical conductivity for samples PBM4 and PBM5 are 1.8787 S/m and 2.0320 S/m, respectively. The measured values range between 1.2492–2.0320 S/m which are within the practical range (0.00001–0.001 S/m) for microwave attenuation applications thus making the synthesized composites promising for shielding applications [15].

Composites PBM1, PBM2, PBM3, PBM4 and PBM5 were then evaluated in terms of their electromagnetic interference (EMI) shielding performance at Ku-band (12.4–18 GHz) by using a waveguide setup connected to a two-port network analyzer. A suitable constant to gauge the shielding performance of a material is the shielding effectiveness (SE), defined as $\text{SE (dB)} = -10 \log(P_t/P_i)$, where P_t and P_0 are defined as the transmitted and initial incident powers, respectively. It is the

combined effect of three shielding mechanisms, shielding by absorption, SE_A , reflection, SE_R , and multiple reflections, SE_M , and is represented by $SE = SE_A + SE_R + SE_M$. The network analyzer measurement is expressed in terms of the S -parameter, S_{11} , S_{21} , S_{12} , and S_{22} , which leads to the reflection coefficient, R , and transmission coefficient, T , with $R = |E_r/E_i|^2 = |S_{11}|^2 = |S_{22}|^2$ and $T = |E_t/E_i|^2 = |S_{21}|^2 = |S_{12}|^2$. If the initial incident electromagnetic wave energy is defined as 1 (full power), the absorption coefficient, A , can be obtained by $A = 1 - R - T$. The effect of multiple reflections between both material surfaces is negligible when the absorption value is large, which then allows the relative intensity of the EM wave energy travelling inside the material to be expressed as $1 - R$. This allows us to obtain the effective absorbance, that is the amount of energy absorbed relative to energy passing through the material, A_{eff} , through $A_{eff} = (1 - R - T)/(1 - R)$ [16–18]. Therefore, SE_R and SE_A

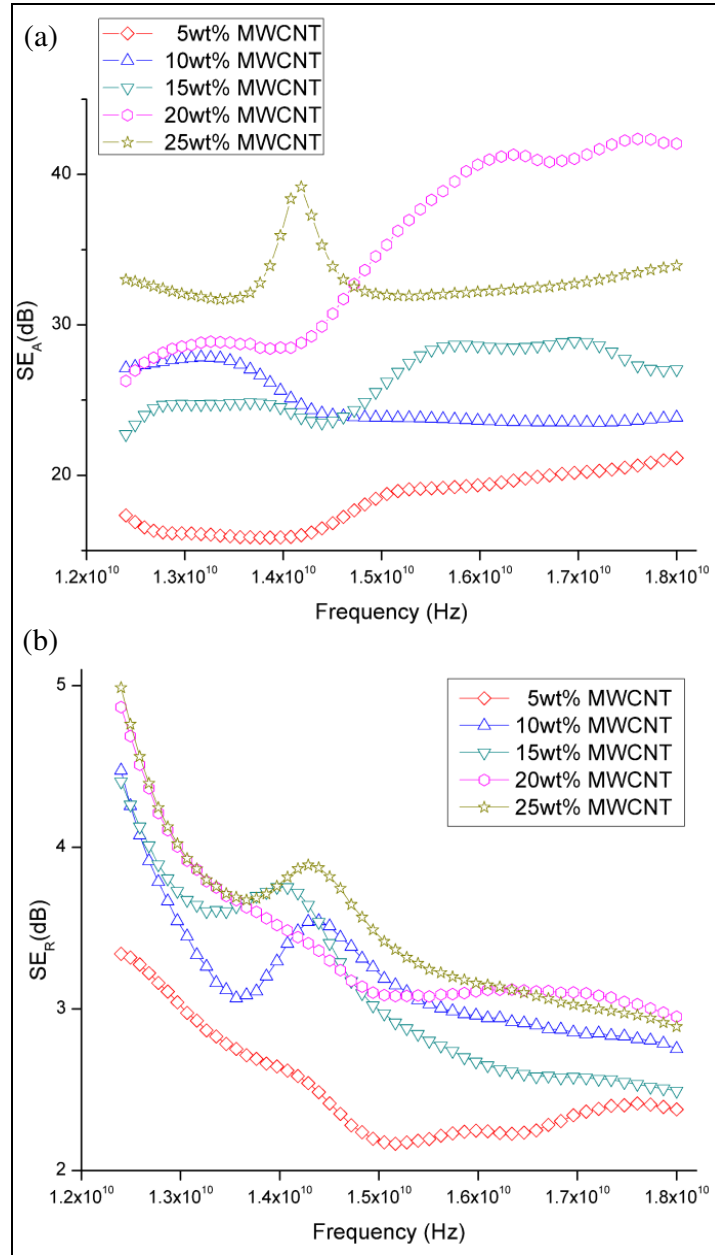


Figure 4. The shielding effectiveness performance due to (a) absorption and (b) reflection with respect to frequency.

can finally be expressed as $SE_R = -10 \log(1 - R)$ and $SE_A = -10 \log(1 - A_{eff}) = -10 \log(T/(1 - R))$.

Figures 4(a) and 4(b) illustrate the different EMI shielding effectiveness exhibited by the different synthesized composites. The shielding performances of the materials can be evaluated by separating it into two frequency ranges; 12.4–14.7 GHz and 14.7–18 GHz. As shown in Figure 4, at frequencies between 12–14.7 GHz, optimum shielding performance for both shielding mechanisms was shown by composite PBM5. For SE_A , sample PBM5 exhibited a minimum value of shielding of 31.7 dB in the first frequency range with a resonance peak reaching a value as high as 39.18 dB at 14.18 GHz. While the increasing amount of MWCNT generally leads to increased absorbing performance for the composites, there was a slight decrease in the value of SE_A for PBM3 compared with PBM2. An opposite trend was observed when comparing between the SE_R for PBM2 and PBM3 at this frequency range where PBM2 exhibited a higher SE_R value than PBM3. For SE_R , the increase of MWCNT wt% leads to a consistent increase in the shielding performance. The highest value of SE_R was observed in sample PBM5 with a value of 4.99 dB at 12.4 GHz.

Samples PBM1, PBM2, PBM3 and PBM4 showed a steady increase in the magnitude of SE_A with each increase in MWCNT wt% before a drop in value was seen for sample PBM5 at frequencies between 14.7–18 GHz. This suggests a threshold for the MWCNT loading for this operating frequency range. The highest value of SE_A was exhibited by sample PBM4 with the value of 42.37 dB at 17.60 GHz. The SE_R values at 14.7–18 GHz show similar trends to that of SE_A at 12–14.7 GHz, where the values generally increase for all samples with respect to the MWCNT wt%, but experience a slight drop when the MWCNT wt% loading increases from 10wt% (PBM2) to 15wt% (PBM3). Due to the significantly larger values of SE_A (up to 8 times higher), than SE_R , it can be concluded that the main mechanism of shielding for the synthesized composites is through absorption of the electromagnetic wave energy transmitting through the shielding material.

4. CONCLUSION

A shielding material based on the composite of BaFe₁₂O₁₉, MWCNT and PANI was synthesized through a facile *in-situ* polymerization method. The XRD patterns reveal prominent peaks corresponding to the crystalline BaFe₁₂O₁₉. FESEM images at several focus sites reveal that the constituents of the composite are randomly distributed between each other with MWCNT and BaFe₁₂O₁₉ acting as the nucleation site for the polyaniline polymerization process. The increment in the MWCNT wt% leads to the increase of the composite's conductivity. Significant values of shielding effectiveness were exhibited by the composites with values as high as 42.37 dB at 17.60 GHz, and the main shielding mechanism of the synthesized composites was found to be absorption, SE_A , due to the significantly larger magnitude than the shielding through reflection, SE_R . Due to the significant values of shielding effectiveness, with values of SE_A more than 10 dB (more than 90% power loss) for all samples, it can be concluded that the proposed composite is a suitable candidate to be used as shielding material in various applications.

ACKNOWLEDGMENT

The authors acknowledge the support from Universiti Teknologi Petronas (UTP) and Universiti Malaysia Perlis (UNIMAP) in terms of providing the necessary facilities and technical support facilitating the completion of this research work.

REFERENCES

1. Tong, X. C., *Advanced Materials and Design for Electromagnetic Interference Shielding*, Taylor & Francis, 2008.
2. Xu, P., X. Han, and M. Wang, "Synthesis and magnetic properties of BaFe₁₂O₁₉ hexaferrite nanoparticles by a reverse microemulsion technique," *The Journal of Physical Chemistry C*, Vol. 111, 5866–5870, 2007.
3. Liu, J., P. Liu, X. Zhang, D. Pan, P. Zhang, and M. Zhang, "Synthesis and properties of single domain sphere-shaped barium hexa-ferrite nano powders via an ultrasonic-assisted co-precipitation route," *Ultrasonics Sonochemistry*, 2014.

4. Hibst, H., "Hexagonal ferrites from melts and aqueous solutions, magnetic recording materials," *Angewandte Chemie International Edition in English*, Vol. 21, 270–282, 1982.
5. Lotgering, F. K., P. R. Locher, and R. P. van Staple, "Anisotropy of hexagonal ferrites with M, W and Y structures containing Fe_{3+} and Fe_{2+} as magnetic ions," *Journal of Physics and Chemistry of Solids*, Vol. 41, 481–487, 1980.
6. Albanese, G., A. Deriu, and S. Rinaldi, "Sublattice magnetization and anisotropy properties of $\text{Ba}_3\text{Co}_2\text{Fe}_{24}\text{O}_{41}$ hexagonal ferrite," *Journal of Physics C: Solid State Physics*, Vol. 9, 1313, 1976.
7. Chiang, J.-C. and A. G. MacDiarmid, "'Polyaniline': Protonic acid doping of the emeraldine form to the metallic regime," *Synthetic Metals*, Vol. 13, 193–205, 1986.
8. Rout, T. K., G. Jha, A. K. Singh, N. Bandyopadhyay, and O. N. Mohanty, "Development of conducting polyaniline coating: A novel approach to superior corrosion resistance," *Surface and Coatings Technology*, Vol. 167, 16–24, 2003.
9. McAndrew, T. P., S. A. Miller, A. G. Gilicinski, and L. M. Robeson, "Poly (aniline) in corrosion resistant coatings," *American Chemical Society*, Washington, DC, United States, 1996.
10. Han, M. and L. Deng, "High frequency properties of carbon nanotubes and their electromagnetic wave absorption properties," J. M. Marulanda, editor, *Carbon Nanotubes Applications on Electron Devices*, InTech, 2011.
11. Qin, F. and C. Brosseau, "A review and analysis of microwave absorption in polymer composites filled with carbonaceous particles," *Journal of Applied Physics*, Vol. 111, 061301, 2012.
12. Li, Y., Y. Huang, S. Qi, L. Niu, Y. Zhang, and Y. Wu, "Preparation, magnetic and electromagnetic properties of polyaniline/strontium ferrite/multiwalled carbon nanotubes composite," *Applied Surface Science*, Vol. 258, 3659–3666, 2012.
13. Goldman, A., *Modern Ferrite Technology*, Springer Science & Business Media, 2006.
14. Rana, U., S. Mondal, J. Sannigrahi, P. K. Sukul, M. A. Amin, S. Majumdar, et al., "Aromatic bi-, tri- and tetracarboxylic acid doped polyaniline nanotubes: Effect on morphologies and electrical transport properties," *Journal of Materials Chemistry C*, Vol. 2, 3382–3389, 2014.
15. Nalwa, H. S., *Handbook of Organic Conductive Molecules and Polymers, Volume 4, Conductive Polymers: Transport, Photophysics and Applications*, Wiley, 1997.
16. Saini, P., V. Choudhary, B. P. Singh, R. B. Mathur, and S. K. Dhawan, "Enhanced microwave absorption behavior of polyaniline-CNT/polystyrene blend in 12.4–18.0 GHz range," *Synthetic Metals*, Vol. 161, 1522–1526, 2011.
17. Phan, C. H., M. Mariatti, and Y. H. Koh, "Electromagnetic interference shielding performance of epoxy composites filled with multiwalled carbon nanotubes/manganese zinc ferrite hybrid fillers," *Journal of Magnetism and Magnetic Materials*, Vol. 401, 472–478, 2016.
18. Wang, Z., G. Wei, and G. L. Zhao, "Enhanced electromagnetic wave shielding effectiveness of Fe doped carbon nanotubes/epoxy composites," *Applied Physics Letters*, Vol. 103, 183109, 2013.